

# Experimental investigation on flow characteristics of deionized water in microtubes

XU ShaoLiang<sup>†</sup>, YUE XiangAn & HOU JiRui

Enhanced Oil Recovery Research Center, China University of Petroleum, Beijing 102249, China

**The flow characteristics of deionized water in microtubes with diameters ranging from 2 to 30  $\mu\text{m}$  are investigated. The experimental results show that the flow characteristics in microtubes with diameters of 16  $\mu\text{m}$  and larger ones are in agreement with the classical theory. However, as the diameters are decreased to 5 and 2  $\mu\text{m}$ , the nonlinear flow characteristics prevail and the results indicate significant departure of flow characteristics from the predictions of the conventional theory, and the smaller the diameters, the larger the departure. As the Reynolds number increases, the degree of nonlinear flow characteristics decrease gradually and the experimental results are approximately equal to the theoretical expectation. The minimum Reynolds number in this study is only  $2.46 \times 10^{-5}$ .**

microtubes, flow characteristics, microscale effect, friction factor ratio, boundary layer fluid

Over the past years, significant attention has been given to liquid flow on the microscale due to the incessant development of micro-electro-mechanical systems (MEMS). As the characteristic lengths are reduced to the same order of magnitude as the hydrodynamic boundary layer thickness, the equations from the conventional theory are not applicable any longer. Several effects such as the size effect and surface effect, which are normally neglected on the macroscale, become more and more important, and even become the dominant influencing factors. The experiments on microscale flow of gases are very reproducible and consistent with the theoretical explanation. However, the microscale flow characteristics of liquids are much more complicated<sup>[1]</sup> because the liquid is incompressible and the resistance caused by viscosity is obvious. In addition, a number of influencing factors such as the intense momentum exchange, the molecular attraction and intermolecular interaction, and the liquid-solid interaction and adhesion also play important roles in the microscale flow of liquids.

Many researchers have conducted experiments on the flow of single-phase fluid in microchannels. The experiments involved different test fluids and microchannels with different cross-sectional shapes. The current

available experimental results are broken into two major groups: one is in agreement with conventional theory and the other deviates from it. Some experimental results which are in agreement with classical theory are shown as follows: Jiang et al.<sup>[2]</sup> studied the variation of the Darcy friction factor with Reynolds number in microtubes with diameters ranging from 8 to 42  $\mu\text{m}$ . The experimental results were in general agreement with the predictions from conventional equations with range of Reynolds number being 0.032–26.1. Li et al.<sup>[3]</sup> studied experimentally the flow characteristics of water and several organic liquids in microtube which was about 25  $\mu\text{m}$  in diameter. They reported that the flow approximately followed the Hagen-Poiseuille theory and the Reynolds number was less than 8. Bucci et al.<sup>[4]</sup> investigated the flow characteristics of water in microtubes with diameters ranging from 172 to 520  $\mu\text{m}$ . Gan et al.<sup>[5]</sup> studied the flow of water and methanol in microchannel with hydraulic diameter of 155.3  $\mu\text{m}$ . Celata et al.<sup>[6]</sup>

Received September 13, 2006; accepted November 14, 2006

doi: 10.1007/s11434-007-0118-z

<sup>†</sup>Corresponding author (email: shaoliang2599@126.com)

Supported by the National Natural Science Foundation of China (Grant No. 50574060) and the National Basic Research Program of China (Grant No. 2002CCA00700)

studied the flow characteristics of water in microtubes with diameters of 30–326  $\mu\text{m}$ . All these experimental results were in rough agreement with the conventional theory.

Some experimental results that deviate from the conventional theory are shown as follows: Pfahler et al.<sup>[7]</sup> conducted experimental studies on isopropanol in rectangular microchannels which were approximately 100  $\mu\text{m}$  wide with depth less than 40  $\mu\text{m}$ , finding the viscosity of liquid decrease. Mala and Li<sup>[8]</sup> investigated water flow in microtubes made of fused silica and stainless steel, with the maximum Reynolds number reaching 2500 and their results indicated that the relationship between Reynolds number and pressure gradient deviated from predictions of conventional theory when the diameter was less than 150  $\mu\text{m}$ . Hao et al.<sup>[9]</sup> investigated water flow in trapezoidal silicon microchannel with a hydraulic diameter of 237  $\mu\text{m}$ , with the relationship between Reynolds number and pressure gradient deviating from the linear behavior and the deviation depending on the Reynolds number.

As can be seen from the experimental results mentioned above, the conclusions are inconsistent under different experimental conditions. The size of microchannels and the Reynolds numbers in previous publications are large, because the researchers mainly focused on the early transition from laminar flow to turbulent flow, and on the different critical Reynolds numbers on the microscale from that on the macroscale. But in the

microflow at low velocity, the liquid-solid interaction is much stronger, which maybe enhances the microscale effect. In this study, we carried out an experiment on the flow characteristics of deionized water in quartz microtubes with minimum diameter as small as 2  $\mu\text{m}$ . The minimum Reynolds number in this study was only  $2.46 \times 10^{-5}$ , which enriches the experimental results. The microscale flow effects are obtained and some new findings have been achieved.

## 1 Experimental apparatus and method

### 1.1 Materials

The microtubes used in this study are naturally fused quartz microtubes (Polymicro Technology Company, USA) with internal diameters of 30, 20, 16, 5 and 2  $\mu\text{m}$ , respectively. The working fluid is deionized water.

### 1.2 Experimental apparatus

The experimental apparatus is shown in Figure 1. The apparatus consists of three parts: the power system, the filter system and the measurement system.  $\text{N}_2$  from the compressed nitrogen gas tank flows through the flow control valve and enters the pressure-buffering reservoir where it drives the deionized water to pass through the three-way pipe to the microtube. The measuring pipe is connected to the test microtube on the other end.

### 1.3 Experimental method

1.3.1 Pressure measurement. The inlet pressure is

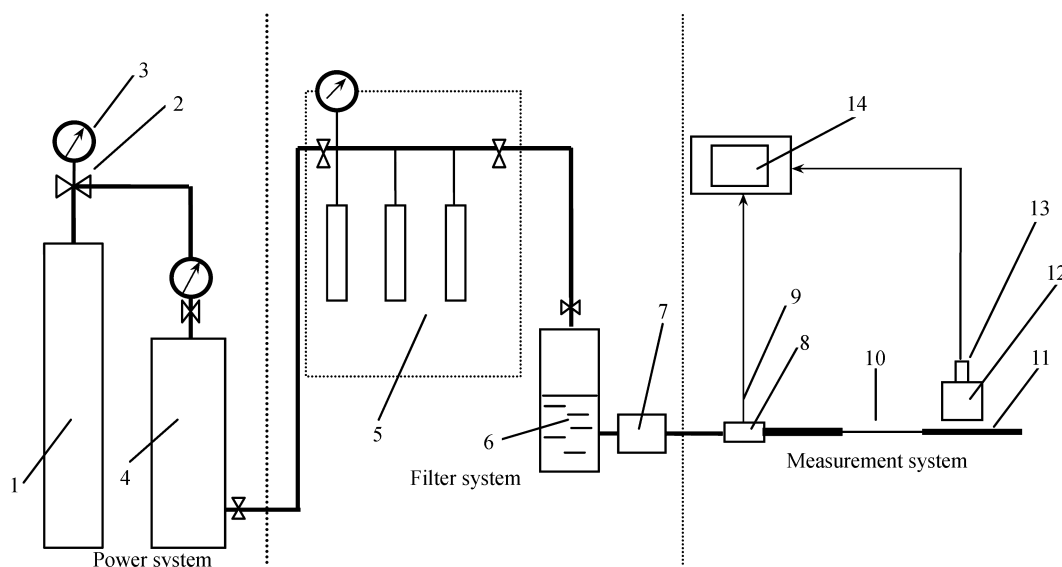


**Figure 1** Experimental apparatus. 1, Compressed nitrogen gas tank; 2, flow control valve; 3, pressure gauge; 4, pressure-buffering reservoir; 5, gas filter; 6, liquid reservoir; 7, liquid filter; 8, three-way pipe; 9, pressure and temperature sensor; 10, microtube; 11, measuring pipe; 12, microscope; 13, real-time image acquisition system; 14, computer.

measured by the pressure sensor with a precision of 0.01 kPa, and is recorded via PC data acquisition system. The flow control valve is turned on slowly to ensure that the pressure rises gradually. For each measurement, it is considered that the flow has reached a steady state when the pressure value does not change any further.

**1.3.2 Flow rate measurement.** Flow rate is measured by the displacement method. A PC image acquisition system is employed to transmit the interfacial image into a computer to record the displacement. The experimental flow rate is calculated using the displacement and the time. Given the small flow rate, and the effect of liquid evaporation, the end of measuring pipe is sealed with unvolatile white oil to keep the interface away from the atmosphere.

**1.3.3 Viscosity measurement.** As a function of temperature, viscosity changes with temperature. In this study, the viscosity of deionized water under standard temperature is obtained from the Handbook of Chemistry. The viscosities under other temperatures are measured by a HAAKE-RS600 rheometer.

## 2 Error analysis

### 2.1 Error of viscosity due to temperature and pressure

Due to the high specific area of the microtube and ability of heat exchange, viscosity is highly sensitive to temperature variation. The integrated temperature controlling method is adopted to reduce the error caused by local temperature controlling. The viscosity variation is  $\pm 2.4\%$  as the temperature varies by  $\pm 1^\circ\text{C}$  at  $25^\circ\text{C}$ . During the course of the experiment, the temperature variation is  $\pm 0.5^\circ\text{C}$ . Thus, the uncertainty of viscosity caused by temperature variation is about  $\pm 1.2\%$ .

Under atmospheric pressure, the viscosity of water increases by about  $0.1\% - 0.3\%$  as pressure increases by every 0.1 MPa. The measuring pressure range in this study is  $0 - 1$  MPa, which results in  $1\% - 3\%$  increase in

viscosity.

### 2.2 Error of flow rate

The measuring displacement in this study is longer than 1 mm with a precision of  $1\ \mu\text{m}$ , so the error is  $0.1\%$ . The measuring time is longer than 1 minute with a precision of 0.01 s, so the error is about  $0.167\%$ . The length of microtubes is measured by a vernier caliper with a precision of 0.02 mm, and the microtubes used in this study are 20–40 mm in length, so the error is  $0.05\% - 0.1\%$ .

### 2.3 Error due to capillary pressure

The calculation of microscale flow rate is influenced by the self-adsorption phenomena, which is caused by the capillary pressure in tubes. The capillary pressure is given by

$$\Delta P_c = 2\sigma \cos \theta / r, \quad (1)$$

where  $\sigma$  is surface tension,  $\theta$  is contact angle between microtube wall and liquid, and  $r$  is the radius of microtube.

It is assumed that the contact angle between microtube wall and liquid is zero. The surface tension of white oil is  $36.7 \times 10^{-2}$  mN/m. The capillary pressure is calculated to be about 0.459 kPa with eq. (1). The lowest pressure in this study is 4 kPa, which leads the uncertainty of pressure to be up to 11%. Thus, the error caused by capillary pressure cannot be neglected. The error is minimized in the process of data analysis.

### 2.4 Error due to inlet and outlet losses

Figure 2 shows schematic diagram of pipe junction with different diameters from the pressure and temperature sensor to the test microtube and the measuring pipe. It can be seen that the pipeline diameter varies from the pressure and temperature sensor to the measuring pipe. Therefore, the inlet and outlet losses possibly influence the flow rate. In order to account for the error due to inlet and outlet losses, the experiments are conducted by using the tubes which are the same in diameter ( $16\ \mu\text{m}$ ) but different in length (20, 40, 60 mm).

On the macroscale, the frictional pressure drop in

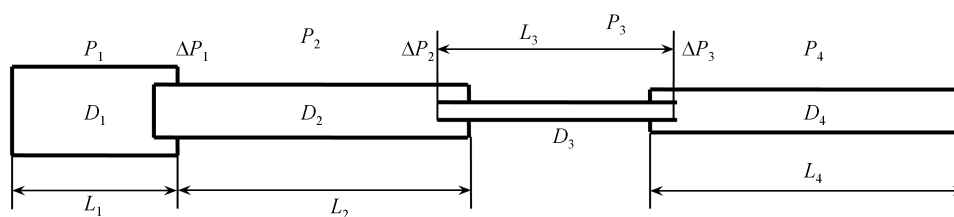


**Figure 2** The schematic diagram of pipe junction with different diameters.

laminar tube flow is expressed as

$$P = f_i \frac{L_i}{D_i} \frac{\rho}{2} v_i^2, \quad i=1, 2, 3, 4. \quad (2)$$

The local pressure drop due to a sudden contraction is

$$\Delta P_i = 0.5 \left( 1 - \frac{D_{i+1}^2}{D_i^2} \right) \frac{\rho}{2} v_i^2, \quad i=1, 2. \quad (3)$$

The local pressure drop due to a sudden enlargement is

$$\Delta P_i = 0.5 \left( 1 - \frac{D_i}{D_{i+1}} \right)^2 \frac{\rho}{2} v_i^2, \quad i=3. \quad (4)$$

The error due to inlet loss, outlet loss and pipe junction pressure drop is

$$\text{Error} = \frac{P_1 + P_2 + P_4 + \Delta P_1 + \Delta P_2 + \Delta P_3}{P_3} \times 100\%. \quad (5)$$

Based on the experimental data, the maximum error due to inlet and outlet losses calculated by eq. (5) is 0.12%. It implies that the error caused by inlet and outlet losses can be neglected.

### 3 Results and discussion

The flow characteristics of deionized water in microtubes (30, 20, 16, 5, 2  $\mu\text{m}$ ) are investigated, and the results are shown as follows.

Figure 3 shows the variation of pressure gradient with Reynolds number for deionized water in different microtubes (30, 20, 16  $\mu\text{m}$ ). The spots represent experimental data and the lines are theoretical values calculated by the Poiseuille equation. Obviously, the experimental results are consistent with theoretical values. It shows that the flow characteristics in microtubes with diameters of 16  $\mu\text{m}$  and larger ones are still in agreement with the conventional theory.

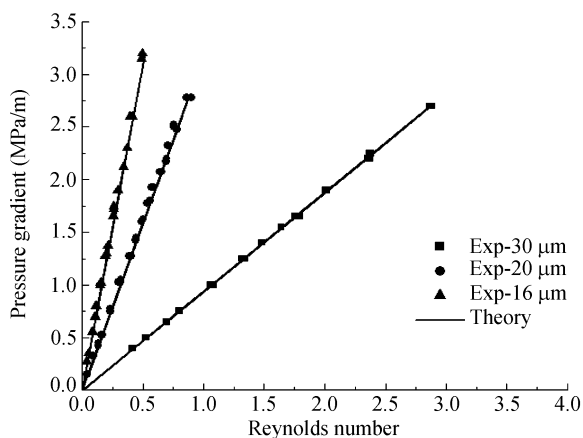


Figure 3 Variation of pressure gradient with  $Re$  (30, 20, 16  $\mu\text{m}$ ).

Figures 4 and 5 show the variation of pressure gradient with Reynolds number for deionized water in microtubes with diameters of 5 and 2  $\mu\text{m}$ , respectively. As shown in these two figures, the experimental data deviate from the theoretical expectation. Furthermore, the deviation in the microtube with a diameter of 2  $\mu\text{m}$  is larger than that of 5  $\mu\text{m}$ . The variation of pressure gradient with Reynolds number shows apparent non-linear flow characteristics, and the flow characteristics deviate from that of the conventional theory. In addition, for the microtube with a diameter of 5  $\mu\text{m}$ , the experimental results are close to the theoretical curve as Reynolds number increases. But when the diameter is decreased to 2  $\mu\text{m}$ , the experimental results deviate from theoretical values as Reynolds number reaches 0.0245. It implies that the smaller the diameter, the stronger the microscale effect.

Due to the microscale effect, the Darcy friction factor

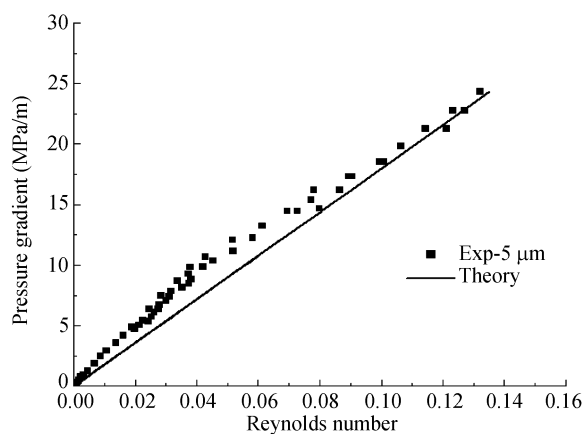


Figure 4 Variation of pressure gradient with  $Re$  (5  $\mu\text{m}$ ).

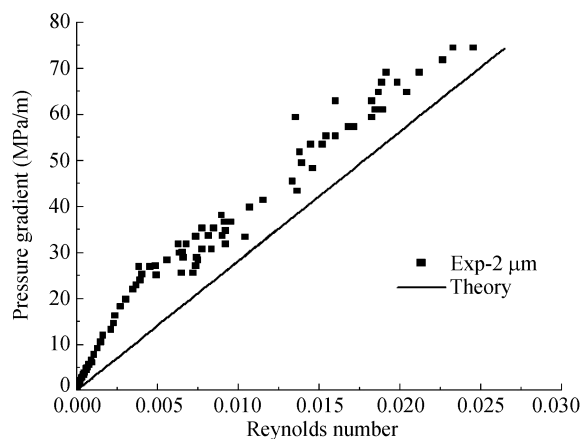


Figure 5 Variation of pressure gradient with  $Re$  (2  $\mu\text{m}$ ).

in microflow deviates from that of conventional theory when single-phase fluid flows in microchannels. In order to account for this discrepancy, the friction factor ratio  $C^*$  is defined as

$$C^* = \frac{f_{\text{exp}}}{f_{\text{H-P}}}, \quad (6)$$

where  $f_{\text{exp}}$  is the friction factor obtained from experimental data, and  $f_{\text{H-P}}$  is the friction factor calculated by the Hagen-Poiseuille equation.

As is evident in Figures 6 and 7, the friction factor ratio  $C^*$  for all the data is greater than 1, and the value of  $C^*$  changes as Reynolds number increases. This indicates that the friction is higher than that predicted by macroscale theory. The maximum  $C^*$  in the microtube with a diameter of 2  $\mu\text{m}$  is about 4.21 while the maximum  $C^*$  in the microtube with a diameter of 5  $\mu\text{m}$  is merely 1.93. As the pressure gradient increases, the  $C^*$  values in the microtube with a diameter of 5  $\mu\text{m}$  begin to accord with the conventional theory, whereas the  $C^*$  values in the microtube with a diameter of 2  $\mu\text{m}$  are still

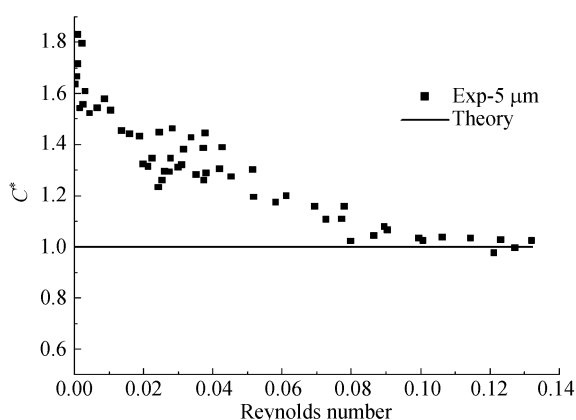


Figure 6 Variation of  $C^*$  with  $Re$  (5  $\mu\text{m}$ ).

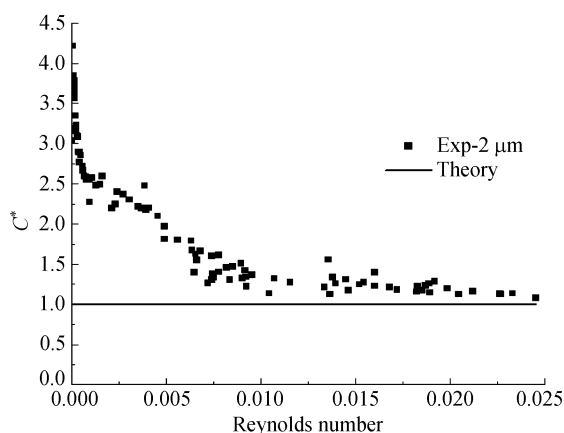


Figure 7 Variation of  $C^*$  with  $Re$  (2  $\mu\text{m}$ ).

20% higher than the theoretical expectation.

In conclusion, the flow characteristics in microtubes with diameters of 16  $\mu\text{m}$  or larger are in agreement with the classical theory. As the diameters decrease to 5 and 2  $\mu\text{m}$ , the experimental results show significant departure from the predictions of conventional theory. Moreover, it implies that the smaller the diameter, the stronger the microscale effect. As Reynolds number increases, the friction factor ratio  $C^*$  decreases, and is approximately equal to the theoretical expectation.

The microflow is affected by a number of factors, such as the surface roughness, the electronic double layer effect and the micropolar effect of fluid molecules. According to laminar fluid theory, the flow characteristics on the macroscale are independent of wall surface roughness which only affects the transition from laminar flow to turbulent flow. However, studies from Mala et al.<sup>[8]</sup> and Li et al.<sup>[10]</sup> showed that the early transition from laminar flow to turbulent flow resulted from wall surface roughness. Thus, it remains unclear whether the laminar flow characteristics are affected by tube wall surface roughness. In addition, as the thickness of electronic double layer reaches the same order of magnitude as characteristic length of the microflow, the ions and potential distribution also influence liquid microflow. Besides, the solid surface property, liquid property and their interaction also contribute to such a process because they largely determine the ions and potential distribution. Ye et al.<sup>[11]</sup> obtained velocity profiles and micro-rotation gyrations in microchannels by a procedure based on numerical method. The results showed that there was an obvious decrease in the flow rate when the coupling between velocity vector and micro-rotation gyration vector was strengthened. As concluded above, the electronic double layer effect and micropolar effect of fluid molecules are the factors that influence microflow.

When liquid flows in a microtube, due to such influencing factors as the electronic double layer effect and the micropolar effect of fluid molecules, intensive interactions occur between the liquid and tube wall. Therefore, evident property difference is shown between the liquid layer adjacent to the solid wall and body fluid. Alexander et al.<sup>[12]</sup> proved theoretically that water density profiles existed in interfacial water layer near to cylinder solid surface, and that the closer to the wall, the higher the density. Liu et al.<sup>[13]</sup> found that the thickness of adsorbed water layer near to solid surface was not a

constant, but a function of the driving pressure gradient. Moreover, it became thinner as pressure gradient increased. Rene et al.<sup>[14]</sup> investigated the meniscus thickness of pure water on fused quartz surface by using an image analyzing interferometer. The results showed that the thickness was larger than 0.1  $\mu\text{m}$ . All these studies clearly showed that the boundary layer fluid played an important role in the microflow.

Since there is a difference between the boundary layer fluid and the body fluid, a small portion of the boundary layer fluid cannot be regarded as the body fluid. Considering the influence of the boundary layer fluid, when the liquids flow in microchannels, the effective flow radius diminishes while the flow resistance increases, which gives rise to the microscale effect and the non-linear flow characteristics. As pressure gradient and wall shear stress increase, the electric double layer effect and the micropolar effect of fluid molecules become weaker. More boundary layer fluid graduates into body fluid and the boundary layer becomes thinner. The effective flow radius increases and the degree of non-linear flow characteristics decreases, which leads to the result that the variation of pressure gradient with

Reynolds number is approximately equal to the theoretical expectation.

## 4 Conclusions

(i) The flow characteristics of deionized water in microtubes with diameters of 16  $\mu\text{m}$  or larger are in agreement with the conventional theory.

(ii) As the diameters are decreased to 5 and 2  $\mu\text{m}$ , the nonlinear flow characteristics prevail and the results indicate significant departure of flow characteristics from the predictions of conventional theory. The friction factor ratio  $C^*$  for the flow in microtubes with diameters of 5 and 2  $\mu\text{m}$  is greater than 1, and the maximum values are 1.93 and 4.21, respectively.

(iii) The values of  $C^*$  for the flow in the microtube with diameter of 2  $\mu\text{m}$  are larger than that of 5  $\mu\text{m}$  at the same Reynolds number. As Reynolds number increases, the degree of nonlinear flow characteristics and the friction factor ratio  $C^*$  decrease. Moreover, the experimental values are approximately equal to the theoretical expectation.

- 1 Liu J. Heat Transfer on Micro/Nano Scale (in Chinese). Beijing: Science Press, 2001
- 2 Jiang X N, Zhou Z Y, Huang X Y, et al. Laminar flow through microchannels used for microscale cooling systems. In: Proceedings of the Electronic Packaging Technology Conference, Singapore, 1997. 119–122
- 3 Li Z H, Zhou X B, Zhu S N. Flow characteristics of non-polar organic liquids with small molecules in a microchannel. Acta Mech Sin (in Chinese), 2002, 34(3): 432–437
- 4 Bucci A, Celata G P, Cumo M, et al. Water single-phase fluid flow and heat transfer in capillary tubes. In: International Conference on Microchannels and Minichannels. Paper 1037 ASME 1, 2003, 319–326
- 5 Gan Y H, Xu J L. Experimental investigation on heat transfer of water and methanol in silicon-based microchannels. Prog Nat Sci (in Chinese), 2005, 15(12): 1498–1503
- 6 Celata G P, Cumo M, Mcphail S, et al. Characterization of fluid dynamic behavior and channel wall effects in microtubes. Intern J Heat Fluid Flow, 2006, 27: 135–143
- 7 Pfahler J, Harley J, Bau H. Gas and liquid flow in small channels. ASME Proc, 1991, 32: 49–60
- 8 Mala G M, Li D Q. Flow characteristics of water in microtubes. Intern J Heat Fluid Flow, 1999, 20(2): 142–148
- 9 Hao P F, He F, Zhu K Q. Flow characteristics in a trapezoidal silicon microchannel. J Micromech Microeng, 2005, 15: 1362–1368
- 10 Li Z X, Du D X, Guo Z Y. Experimental study on flow characteristics of liquid in circular tubes. In: Proceedings of the International Conference on Heat transfer and Transport Phenomena in Microscale, Banff, Canada, 2000. 162–167
- 11 Ye S J, Zhu K Q, Wang W. Laminar flow of micropolar fluid in rectangular microchannels. Acta Mech Sin, 2006, 22(5): 403–408
- 12 Alexander P, Michael G. Water-graphite interaction and behavior of water near the graphite surface. J Phys Chem B, 2004, 108(4): 1357–1364
- 13 Liu D X, Yue X A, Hou J R, et al. Experimental study of adsorbed water layer on solid particle surface. Acta Miner Sin (in Chinese), 2005, 25(1): 15–19
- 14 Rene R M, Wayner P C. Aqueous wetting films on fused quartz. J Coll Interf Sci, 1999, 214(2): 156–169